

# Pseudoscalar boson and SM-like Higgs boson productions at LHC in simplest little Higgs model

Lei Wang, Xiao-Fang Han

*Department of Physics, Yantai University, Yantai 264005, PR China*

## Abstract

In the framework of the simplest little Higgs model (SLHM), we perform a comprehensive study for the pair productions of the pseudoscalar boson  $\eta$  and SM-like Higgs boson  $h$  at LHC, namely  $gg(b\bar{b}) \rightarrow \eta\eta$ ,  $gg(q\bar{q}) \rightarrow \eta h$  and  $gg(b\bar{b}) \rightarrow hh$ . These production processes provide a way to probe the couplings between Higgs bosons. We find that the cross section of  $gg \rightarrow \eta\eta$  always dominates over that of  $b\bar{b} \rightarrow \eta\eta$ . When the Higgs boson  $h$  which mediates these two processes is on-shell, their cross sections can reach several thousand  $fb$  and several hundred  $fb$ , respectively. When the intermediate state  $h$  is off-shell, those two cross sections are reduced by two orders of magnitude, respectively. The cross sections of  $gg \rightarrow \eta h$  and  $q\bar{q} \rightarrow \eta h$  are about in the same order of magnitude, which can reach  $\mathcal{O}(10^2 fb)$  for a light  $\eta$  boson. Besides, compared with the SM prediction, the cross section of a pair of SM-like Higgs bosons production at LHC can be enhanced sizably. Finally, we briefly discuss the observable signatures of  $\eta\eta$ ,  $\eta h$  and  $hh$  at the LHC, respectively.

PACS numbers: 12.60.-i, 12.60.Fr, 14.80.Ec

## I. INTRODUCTION

Little Higgs theory [1] has been proposed as an interesting solution to the hierarchy problem. So far various realizations of the little Higgs symmetry structure have been proposed [2–5], which can be categorized generally into two classes [6]. One class use the product group, represented by the littlest Higgs model [3], in which the SM  $SU(2)_L$  gauge group is from the diagonal breaking of two (or more) gauge groups. The other class use the simple group, represented by the simplest little Higgs model (SLHM) [4], in which a single larger gauge group is broken down to the SM  $SU(2)_L$ .

Since these little Higgs models mainly alter the properties of the Higgs boson, hints of these models may be unraveled from various Higgs boson processes. The phenomenology of Higgs boson in these little Higgs models has been widely studied [7–14]. In addition to the SM-like Higgs boson  $h$ , the SLHM predicts a pseudoscalar boson  $\eta$ , whose mass can be as low as  $\mathcal{O}(10 \text{ GeV})$ . The constraint from the non-observation in the decay  $\Upsilon \rightarrow \gamma\eta$  excludes  $\eta$  with mass below 5-7 GeV [15]. In this paper, we will focus on the pair productions of neutral Higgs bosons at LHC in the SLHM, namely  $gg(b\bar{b}) \rightarrow \eta\eta$ ,  $gg(q\bar{q}) \rightarrow \eta h$  and  $gg(b\bar{b}) \rightarrow hh$ . These production processes at LHC are very important because they will provide a way to probe the couplings of  $h\eta\eta$  and  $hhh$ , and shed light on the Higgs potential. Further, Higg-pair production at LHC may be sensitive to new physics, and it has been studied in many new physics model, such as little Higgs models [13, 14], supersymmetric models [16], models of universal extra dimensions [17] and left-right twin Higgs model [18]. Note that  $gg(b\bar{b}) \rightarrow hh$  process has been studied in [13]. In order to perform a comprehensive study for the pair productions of neutral Higgs bosons at LHC, we reconsider them here.

This work is organized as follows. In Sec. II we recapitulate the SLHM. In Sec. III we study  $gg(b\bar{b}) \rightarrow \eta\eta$ ,  $gg(q\bar{q}) \rightarrow \eta h$  and  $gg(b\bar{b}) \rightarrow hh$  production processes at LHC, respectively. Finally, we give our conclusion in Sec. IV.

## II. SIMPLEST LITTLE HIGGS MODEL

The SLHM is based on  $[SU(3) \times U(1)_X]^2$  global symmetry. The gauge symmetry  $SU(3) \times U(1)_X$  is broken down to the SM electroweak gauge group by two copies of scalar fields  $\Phi_1$  and  $\Phi_2$ , which are triplets under the  $SU(3)$  with aligned VEVs  $f_1$  and  $f_2$ . The uneaten five

pseudo-Goldstone bosons can be parameterized as

$$\Phi_1 = e^{i t_\beta \Theta} \begin{pmatrix} 0 \\ 0 \\ f_1 \end{pmatrix}, \quad \Phi_2 = e^{-\frac{i}{t_\beta} \Theta} \begin{pmatrix} 0 \\ 0 \\ f_2 \end{pmatrix}, \quad (1)$$

where

$$\Theta = \frac{1}{f} \left[ \begin{pmatrix} 0 & 0 \\ 0 & 0 \\ H^\dagger & 0 \end{pmatrix} + \frac{\eta}{\sqrt{2}} \begin{pmatrix} 1 & 0 & 0 \\ 0 & 1 & 0 \\ 0 & 0 & 1 \end{pmatrix} \right], \quad (2)$$

$f = \sqrt{f_1^2 + f_2^2}$  and  $t_\beta \equiv \tan \beta = f_2/f_1$ . Under the  $SU(2)_L$  SM gauge group,  $\eta$  is a real scalar, while  $H$  transforms as a doublet and can be identified as the SM Higgs doublet. The kinetic term in the non-linear sigma model is

$$\mathcal{L}_\Phi = \sum_{j=1,2} \left| \left( \partial_\mu + ig A_\mu^a T^a - i \frac{g_x}{3} B_\mu^x \right) \Phi_j \right|^2, \quad (3)$$

where  $g_x = g \tan \theta_W / \sqrt{1 - \tan^2 \theta_W / 3}$  with  $\theta_W$  being the electroweak mixing angle. As  $\Phi_1$  and  $\Phi_2$  develop their VEVs, the new heavy gauge bosons  $Z'$ ,  $Y^0$ , and  $X^\pm$  get their masses proportional to  $f$ :

$$m_{Z'}^2 = g^2 f^2 \frac{2}{3 - \tan^2 \theta_W}, \quad m_{X^\pm}^2 = m_{Y^0}^2 = \frac{g^2}{2} f^2. \quad (4)$$

The gauged  $SU(3)$  symmetry promotes the SM fermion doublets into  $SU(3)$  triplets. There are two possible gauge charge assignments for the fermions: the 'universal' embedding and the 'anomaly-free' embedding. The first choice is not favored by the electroweak precision data [4], so we focus on the second way of embedding. The quark Yukawa interactions for the third generation and the first two generations can be written respectively as

$$\mathcal{L}_3 = i \lambda_1^t t_1^c \Phi_1^\dagger Q_3 + i \lambda_2^t t_2^c \Phi_2^\dagger Q_3 + i \frac{\lambda_d^m}{\Lambda} d_m^c \epsilon_{ijk} \Phi_1^i \Phi_2^j Q_3^k + h.c., \quad (5)$$

$$\mathcal{L}_{1,2} = i \lambda_1^{d_n} d_{1n}^c Q_n^T \Phi_1 + i \lambda_2^{d_n} d_{2n}^c Q_n^T \Phi_2 + i \frac{\lambda_u^{mn}}{\Lambda} u_m^c \epsilon_{ijk} \Phi_1^{*i} \Phi_2^{*j} Q_n^k + h.c., \quad (6)$$

where  $n = 1, 2$  are the first two generation indices;  $i, j, k = 1, 2, 3$ ;  $Q_3 = \{t_L, b_L, iT_L\}$  and  $Q_n = \{d_{nL}, -u_{nL}, iD_{nL}\}$ ;  $d_m^c$  runs over  $(d^c, s^c, b^c, D^c, S^c)$ ;  $d_{1n}^c$  and  $d_{2n}^c$  are linear combinations of  $d^c$  and  $D^c$  for  $n = 1$  and of  $s^c$  and  $S^c$  for  $n = 2$ ;  $u_m^c$  runs over  $(u^c, c^c, t^c, T^c)$ . For simplicity,

we assume the quark flavor mixing are small and neglect the mixing effects. Eqs. (5) and (6) contain the Higgs boson interactions and the mass terms for the three generations of quarks:

$$\mathcal{L}_t \simeq -f\lambda_2^t [x_\lambda^t c_\beta t_1^c (-s_1 t_L + c_1 T_L) G_1(\eta) + s_\beta t_2^c (s_2 t_L + c_2 T_L) G_2(\eta)] + h.c., \quad (7)$$

$$\mathcal{L}_{d_n} \simeq -f\lambda_2^{d_n} [x_\lambda^{d_n} c_\beta d_1^c (s_1 d_{nL} + c_1 D_{nL}) G_1^*(\eta) + s_\beta d_2^c (-s_2 d_{nL} + c_2 D_{nL}) G_2^*(\eta)] + h.c., \quad (8)$$

$$\mathcal{L}_b \simeq -\frac{\lambda_b}{\Lambda} f^2 s_\beta c_\beta s_3 b^c b_L G_3(\eta) + h.c., \quad (9)$$

$$\mathcal{L}_q \simeq -\frac{\lambda_q}{\Lambda} f^2 s_\beta c_\beta s_3 q^c q_L G_3^*(\eta) + h.c. \quad (q = u, c), \quad (10)$$

where

$$\begin{aligned} x_\lambda^t &\equiv \frac{\lambda_1^t}{\lambda_2^t}, \quad x_\lambda^{d_n} \equiv \frac{\lambda_1^{d_n}}{\lambda_2^{d_n}}, \quad s_\beta \equiv \frac{f_2}{\sqrt{f_1^2 + f_2^2}}, \quad c_\beta \equiv \frac{f_1}{\sqrt{f_1^2 + f_2^2}}, \\ s_1 &\equiv \sin \frac{t_\beta(h+v)}{\sqrt{2}f}, \quad s_2 \equiv \sin \frac{(h+v)}{\sqrt{2}t_\beta f}, \quad s_3 \equiv \sin \frac{(h+v)(t_\beta^2 + 1)}{\sqrt{2}t_\beta f}, \\ G_1(\eta) &\equiv 1 - i \frac{t_\beta}{\sqrt{2}f} \eta - \frac{t_\beta^2}{4f^2} \eta^2, \quad G_2(\eta) \equiv 1 + i \frac{1}{\sqrt{2}t_\beta f} \eta - \frac{1}{4t_\beta^2 f^2} \eta^2, \\ G_3(\eta) &\equiv 1 + i \frac{1}{\sqrt{2}f} (t_\beta - \frac{1}{t_\beta}) \eta - \frac{1}{4f^2} (t_\beta - \frac{1}{t_\beta})^2 \eta^2, \end{aligned} \quad (11)$$

with  $h$  and  $v$  being the SM-like Higgs boson field and its VEV, respectively. The mass eigenstates are obtained by mixing the corresponding interaction eigenstates, e.g., the mass eigenstates  $(t_{mL}, T_{mL})$  and  $(t_m^c, T_m^c)$  are respectively the mixtures of  $(t_L, T_L)$  and  $(t^c, T^c)$ . The diagonalization of the mass matrix in Eqs. (7) and (8) is performed numerically in our analysis, and the relevant couplings of  $h$  and  $\eta$  bosons can also be obtained without resort to any expansion of  $v/f$ . Hereafter we denote the mass eigenstates without the subscript 'm' for simplicity.

The Yukawa and gauge interactions break the global symmetry and then provide a potential for the Higgs boson. However, the Coleman-Weinberg potential alone is not sufficient since the generated  $h$  mass is too heavy and the new pseudoscalar  $\eta$  is massless. Therefore, one can introduce a tree-level  $\mu$  term which can partially cancel the  $h$  mass [4, 10]:

$$-\mu^2(\Phi_1^\dagger \Phi_2 + h.c.) = -2\mu^2 f^2 s_\beta c_\beta \cos \left( \frac{\eta}{\sqrt{2}s_\beta c_\beta f} \right) \cos \left( \frac{\sqrt{H^\dagger H}}{f c_\beta s_\beta} \right). \quad (12)$$

The Higgs potential becomes

$$V = -m^2 H^\dagger H + \lambda(H^\dagger H)^2 - \frac{1}{2} m_\eta^2 \eta^2 + \lambda' H^\dagger H \eta^2 + \dots, \quad (13)$$

where

$$m^2 = m_0^2 - \frac{\mu^2}{s_\beta c_\beta}, \quad \lambda = \lambda_0 - \frac{\mu^2}{12s_\beta^3 c_\beta^3 f^2}, \quad \lambda' = -\frac{\mu^2}{4f^2 s_\beta^3 c_\beta^3}, \quad (14)$$

with  $m_0$  and  $\lambda_0$  being respectively the one-loop contributions to the  $h$  mass and the quartic couplings from the contributions of fermion loops and gauge boson loops [4]. The Higgs VEV and the masses of  $h$  and  $\eta$  are given by

$$v^2 = \frac{m^2}{\lambda}, \quad m_h^2 = 2m^2, \quad m_\eta^2 = \frac{\mu^2}{s_\beta c_\beta} \cos\left(\frac{v}{\sqrt{2}f s_\beta c_\beta}\right). \quad (15)$$

The Coleman-Weinberg potential involves the following parameters:

$$f, x_\lambda^t, t_\beta, \mu, m_\eta, m_h, v. \quad (16)$$

Due to the modification of the observed  $W$  gauge boson mass,  $v$  is defined as [10]

$$v \simeq v_0 \left[ 1 + \frac{v_0^2}{12f^2} \frac{t_\beta^4 - t_\beta^2 + 1}{t_\beta^2} - \frac{v_0^4}{180f^4} \frac{t_\beta^8 - t_\beta^6 + t_\beta^4 - t_\beta^2 + 1}{t_\beta^4} \right], \quad (17)$$

where  $v_0 = 246$  GeV is the SM Higgs VEV. Assuming that there are no large direct contributions to the potential from physics at the cutoff, we can determine other parameters in Eq. (16) from  $f, t_\beta$  and  $m_\eta$  ( $m_h$ ) with the definition of  $v$  in Eq. (17).

### III. $\eta\eta, \eta h$ AND $hh$ PRODUCTIONS AT LHC

At the LHC the double  $\eta$  production can proceed through gluon-gluon fusion and  $b\bar{b}$  annihilation, as shown in Fig. 1 and Fig. 2, respectively. Since their Yukawa couplings are very small, we do not consider the contributions of  $q\bar{q}$  ( $q = u, c, d, s$ ) annihilation processes. For the gluon-gluon fusion process, there are two types of Feynman diagrams. One is the triangle diagrams where an off-shell (or on-shell)  $h$  boson, produced from gluon-gluon fusion through the heavy quark loops, decays into a pair of  $\eta$  bosons. The other is the box diagrams where the double  $\eta$  bosons are produced through quark boxes. Due to the large Yukawa couplings of the heavy quarks and the large parton distribution function of gluon at the LHC, the contributions of the gluon-gluon fusion process can dominate over those of  $b\bar{b}$  annihilation process. The Feynman diagrams of  $gg(b\bar{b}) \rightarrow hh$  process can be obtained from those of  $gg(b\bar{b}) \rightarrow \eta\eta$  by replacing the final state two  $\eta$  bosons with two  $h$  bosons.

The  $\eta h$  associated production at LHC can proceed through gluon-gluon fusion and  $q\bar{q}$  annihilation, as shown in Fig. 3 and Fig. 4. In addition to the diagrams which are similar

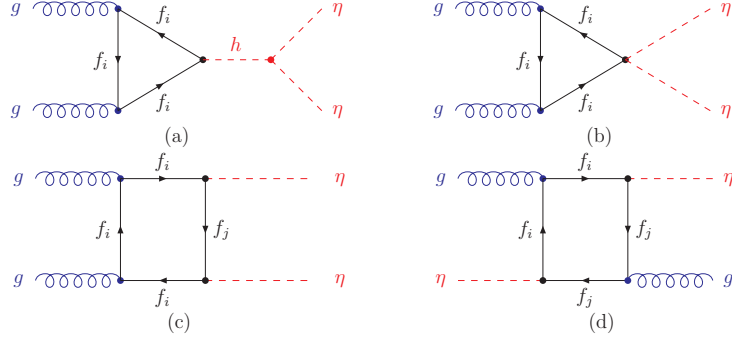


FIG. 1: Feynman diagrams for double  $\eta$  production via gluon-gluon fusion in the SLHM. Here  $i, j = 1, 2$  with  $(f_1, f_2)$  denoting  $(t, T)$  or  $(d, D)$  or  $(s, S)$ . The diagrams by exchanging the two gluons or exchanging the two  $\eta$  bosons in (c,d) are not shown here.

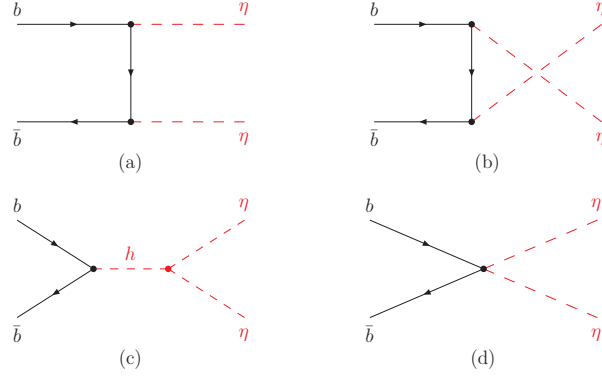


FIG. 2: Feynman diagrams for double  $\eta$  production via  $b\bar{b}$  annihilation in the SLHM.

to those of  $\eta\eta$  production, there are some Feynman diagrams where  $Z$  and  $Z'$ , produced from gluon-gluon fusion through the quark loops and from  $q\bar{q}$  annihilation, decay into  $\eta h$  as shown in Fig. 3(a) and Fig. 4(a), respectively. Although the new neutral gauge boson  $Y^0$  can also contribute to the processes  $gg \rightarrow \eta h$  and  $q\bar{q} \rightarrow \eta h$ , its gauge coupling is suppressed by  $v/f$  and  $1/t_\beta$  [6, 11]. Therefore, we neglect the contributions of  $Y^0$ .

The calculations of the loop diagrams in Fig. 1 and Fig. 3 are straightforward. Each loop diagram is composed of some scalar loop functions [19] which are calculated by using LoopTools [20]. The amplitudes of triangle diagrams are as follows:

$$\begin{aligned}
M_{1(a)} + M_{1(b)} &= \frac{\delta^{ab} g_s^2}{4\pi^2} \epsilon_1^a(k_1) \cdot \epsilon_2^b(k_2) \sum_f m_f (1 + 2m_f^2 C_0 - k_1 \cdot k_2 C_0) \left( \frac{g_{h\bar{f}f} \cdot g_{h\eta\eta}}{\hat{s} - m_h^2 + im_h \Gamma_h} + g_{\eta\eta\bar{f}f} \right), \\
M_{3(b)} + M_{3(c)} &= \frac{\delta^{ab} g_s^2}{4\pi^2} \epsilon_1^\mu(k_1) \epsilon_2^\nu(k_2) k_1^\beta k_2^\alpha \varepsilon_{\mu\alpha\nu\beta} \sum_f m_f C_0 \left( \frac{g_{\eta\bar{f}f} \cdot g_{h\eta\eta}}{\hat{s} - m_\eta^2} + g_{h\eta\bar{f}f} \right),
\end{aligned} \tag{18}$$

where  $\hat{s} = k^2 = (k_1 + k_2)^2$ .  $M_{x(y)}$  denotes the amplitude of Fig.  $x(y)$  with  $x = 1, 3$  and

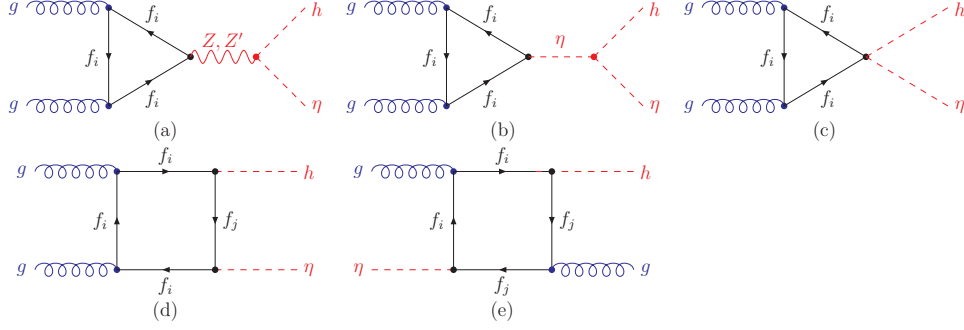


FIG. 3: Feynman diagrams for  $\eta h$  associated production via gluon-gluon fusion in the SLHM. For (b-e),  $i, j = 1, 2$  with  $(f_1, f_2)$  denoting  $(t, T)$  or  $(d, D)$  or  $(s, S)$ ; For (a),  $f_i$  denotes the SM quarks and new quarks  $T$ ,  $D$  and  $S$ . The diagrams by exchanging the two gluons or exchanging the  $\eta$  and  $h$  bosons in (d,e) are not shown here.

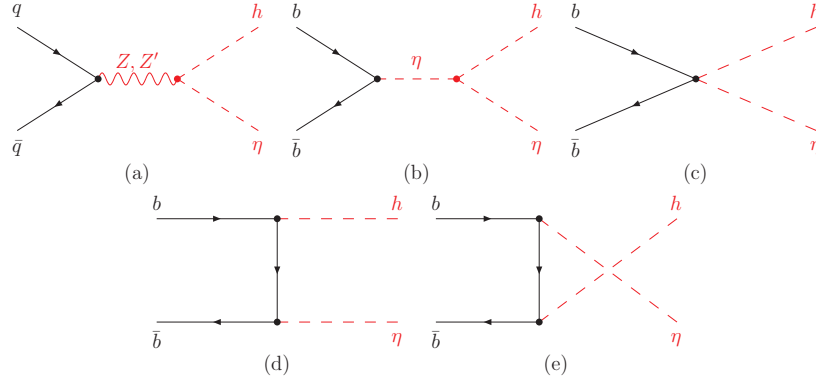


FIG. 4: Feynman diagrams for  $\eta h$  associated production via  $b\bar{b}$  annihilation in the SLHM. The parton  $q$  in (a) denotes  $u$ ,  $c$ ,  $d$ ,  $s$ ,  $b$ .

$y=a, b, c$ .  $C_0 \equiv C_0(0, 0, \hat{s}, m_f^2, m_f^2, m_f^2)$  is the 3-point Feynman integrals scalar function, and  $a$  and  $b$  denote the color factor of gluons.

$$M_{3(a)} = \frac{-g_{\alpha\beta} + k_\alpha k_\beta / m_Z^2}{\hat{s} - m_Z^2} g_{Z\eta h} (p_h - p_\eta)^\beta \epsilon_{1\mu}(k_1) \epsilon_{2\nu}(k_2) \sum_f F^{\alpha\mu\nu}(m_f, g_a^{Z\bar{f}f}) \quad (19)$$

$$+ \frac{-g_{\alpha\beta} + k_\alpha k_\beta / m_{Z'}^2}{\hat{s} - m_{Z'}^2 + im_{Z'} \Gamma_{Z'}} g_{Z'\eta h} (p_h - p_\eta)^\beta \epsilon_{1\mu}(k_1) \epsilon_{2\nu}(k_2) \sum_f F^{\alpha\mu\nu}(m_f, g_a^{Z'\bar{f}f}). \quad (20)$$

$F^{\alpha\mu\nu}(m_f, g_a^{Z\bar{f}f})$  is the effective coupling of  $ggZ$  [21, 22]:

$$F^{\alpha\mu\nu} = \sum_Q \frac{g_a g_s^2 \text{Tr}[T^a T^b]}{4\pi^2} [\varepsilon^{\mu\nu\omega\varphi} k_{1\omega} k_{2\varphi} k^\alpha F_1(\hat{s}) + (\varepsilon^{\alpha\mu\omega\varphi} k_2^\nu - \varepsilon^{\alpha\nu\omega\varphi} k_1^\mu) k_{1\omega} k_{2\varphi} F_2(\hat{s}) \quad (21)$$

$$+ (\varepsilon^{\alpha\mu\omega\varphi} k_1^\nu - \varepsilon^{\alpha\nu\omega\varphi} k_2^\mu) k_{1\omega} k_{2\varphi} F_3(\hat{s}) + \varepsilon^{\alpha\mu\nu\omega} (k_{1\omega} - k_{2\omega}) F_4(\hat{s})]$$

where  $g_a$  is the coupling of axial vector current and  $F_i(\hat{s})$  ( $i = 1 - 4$ ) are scalar functions,

$$\begin{aligned} F_1 &= -\frac{1}{\hat{s}}(B_0[0, m_f^2, m_f^2] - B_0[\hat{s}, m_f^2, m_f^2] + 1 + 2C_0[0, 0, \hat{s}, m_f^2, m_f^2, m_f^2]m_f^2), \\ -F_2 &= F_3 = \frac{2}{\hat{s}} \left[ -\frac{1}{2}(B_0[0, m_f^2, m_f^2] - B_0[\hat{s}, m_f^2, m_f^2] + 1 - 2C_0[0, 0, \hat{s}, m_f^2, m_f^2, m_f^2]m_f^2) + 1 \right], \\ F_4 &= -\frac{1}{2}(B_0[0, m_f^2, m_f^2] - B_0[\hat{s}, m_f^2, m_f^2] + 1 - 2C_0[0, 0, \hat{s}, m_f^2, m_f^2, m_f^2]m_f^2) + 1, \end{aligned} \quad (22)$$

where the unity in  $F_4$  is the anomaly term.

The amplitudes expressions of box diagrams are lengthy, which are not presented here. The hadronic cross section at the LHC is obtained by convoluting the parton cross section with the parton distribution functions. In our calculations we use CTEQ6L [23] to generate the parton distributions with the renormalization scale  $\mu_R$  and the factorization scale  $\mu_F$  chosen to be  $\mu_R = \mu_F = 2m_\eta$  for  $\eta\eta$  production process ( $\mu_R = \mu_F = m_\eta + m_h$  for  $\eta h$  production;  $\mu_R = \mu_F = 2m_h$  for  $hh$  production) and use the two-loop running coupling constant  $\alpha_s$  with  $\alpha_s(m_Z) = 0.118$ . The  $h$  boson mediating  $gg(b\bar{b}) \rightarrow \eta\eta$  and  $Z'$  mediating  $gg(q\bar{q}) \rightarrow \eta h$  can be respectively on-shell for  $m_h \geq 2m_\eta$  and  $m_{Z'} \geq m_\eta + m_h$ . In order to take into account possible resonance effects of  $h$  and  $Z'$ , we have calculated the decay modes of  $h$  and  $Z'$ , which are shown in appendix.

The SM input parameters relevant in our study are taken as  $m_t = 173.3$  GeV [24] and  $m_Z = 91.1876$  GeV [25]. The free SLHM parameters are  $f$ ,  $t_\beta$ ,  $m_\eta$  ( $m_h$ ),  $x_\lambda^d$  and  $x_\lambda^s$ . As shown above, the parameters  $x_\lambda^t$ ,  $\mu$ ,  $m_h$  ( $m_\eta$ ) can be determined by  $f$ ,  $t_\beta$ ,  $m_\eta$  ( $m_h$ ) and  $v$ . To satisfy the bound of LEP2, we require that  $m_h$  is larger than 114.4 GeV [26]. Certainly, due to the presence of the dominant decay mode  $h \rightarrow \eta\eta$  and suppression of  $hZZ$  coupling [9, 10], the LEP2 bound on  $m_h$  should be loosened to some extent. The recent studies about  $Z$  leptonic decay and  $e^+e^- \rightarrow \tau^+\tau^-\gamma$  process at the  $Z$  pole show that the scale  $f$  should be respectively larger than 5.6 TeV and 5.4 TeV, which does not depend on  $t_\beta$  [27]. Such large values of  $f$  can suppress the SLHM predictions sizably. However, the factor  $t_\beta$  in the couplings of  $h$  and  $\eta$  can be taken as a large value to cancel the suppression of  $f$  partially. For the perturbation to be valid,  $t_\beta$  cannot be too large for fixed  $f$ . If we require  $\mathcal{O}(v_0^4/f^4)/\mathcal{O}(v_0^2/f^2) < 0.1$  in the expansion of  $v$ ,  $t_\beta$  should be below 28 for  $f = 5.6$  TeV. In our calculation, we take  $f = 5.6$  TeV and  $t_\beta = 15, 20, 25$ , respectively.

Besides, the SLHM predicts a heavy neutrino for leptons of each generation, and the mixing of the heavy neutrinos with the light neutrinos in conjunction with a family mixing



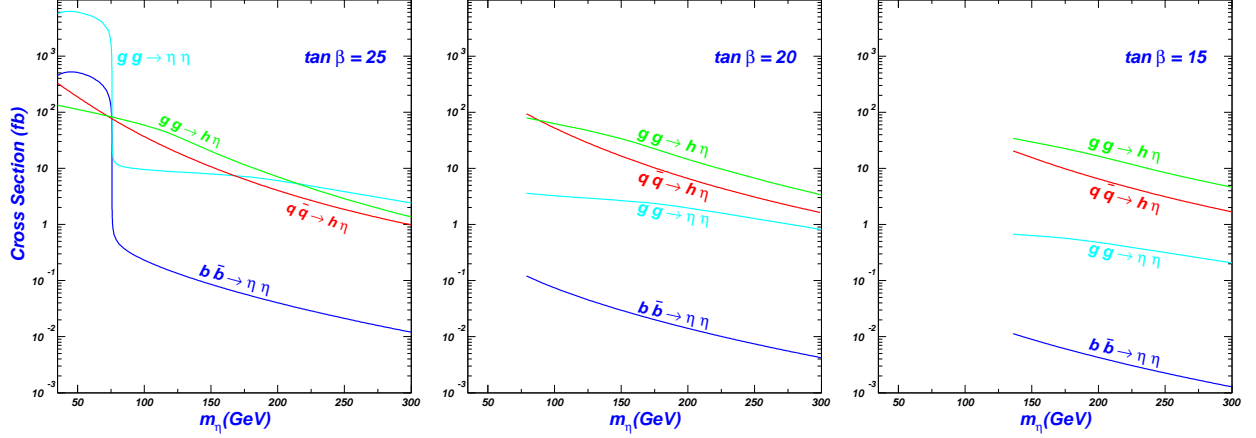


FIG. 5: For  $f = 5.6$  TeV, hadronic cross sections of  $gg(b\bar{b}) \rightarrow \eta\eta$  and  $gg(q\bar{q}) \rightarrow \eta h$  at the LHC versus the  $\eta$  boson mass. The incomplete lines for  $\tan \beta = 20$  and  $15$  show the lower bounds of the  $\eta$  mass, respectively.

in the lepton sectors produces the new lepton mixing matrix  $V_\ell$  [6, 28, 29], which can lead to lepton-flavor violating processes, such as  $\mu \rightarrow e\gamma$ ,  $\mu \rightarrow ee\bar{e}$  and  $\mu N \rightarrow eN$ . The experimental constraints from the three processes are very strong. For example, using only two lepton generations, we need  $f \gtrsim 8$  TeV or very small mixing angles or heavy neutrinos mass splitting, i.e.,  $\sin 2\theta \lesssim 0.01$  or  $\delta \lesssim 1\%$  with  $t_\beta = 1$  [28]. However, as in the quark sector of the SM, this lepton-flavor violation will vanish in the limit that the mixing matrix  $V_\ell$  is diagonal or the masses of the heavy neutrinos are degenerate [6]. In this paper, we assume the two scenarios, so that  $f$  and  $t_\beta$  are free from the experimental constraints of the lepton-flavor violating processes. Note that the parameters of lepton sector, i.e., mixing matrix  $V_\ell$  and masses of the heavy neutrinos, are not involved in our calculations directly.

The small mass of the  $d(s)$  quark requires one of the couplings  $\lambda_1^d$  and  $\lambda_2^d$  ( $\lambda_1^s$  and  $\lambda_2^s$ ) to be very small, so there is almost no mixing between the SM down-type quarks and their heavy partners. We assume  $\lambda_1^d(\lambda_1^s)$  is small, and take  $x_\lambda^d = 1.1 \times 10^{-4}$  ( $x_\lambda^s = 2.1 \times 10^{-3}$ ), which can make the masses of  $D$  and  $S$  be in the range of 1 TeV and 2 TeV for other parameters taken in our calculations. In fact, our results show that different choices of  $x_\lambda^d$  and  $x_\lambda^s$  can not have sizable effects on the result.

In Fig. 5, we plot the hadronic cross sections of  $gg(b\bar{b}) \rightarrow \eta\eta$  and  $gg(q\bar{q}) \rightarrow \eta h$  at the LHC versus the  $\eta$  boson mass, respectively. Fig. 5 shows the cross sections of these processes are all sensitive to the  $\eta$  mass, and the values decrease with increasing of the  $\eta$  mass. For the double  $\eta$  production, the cross section of gluon-gluon fusion process always dominates

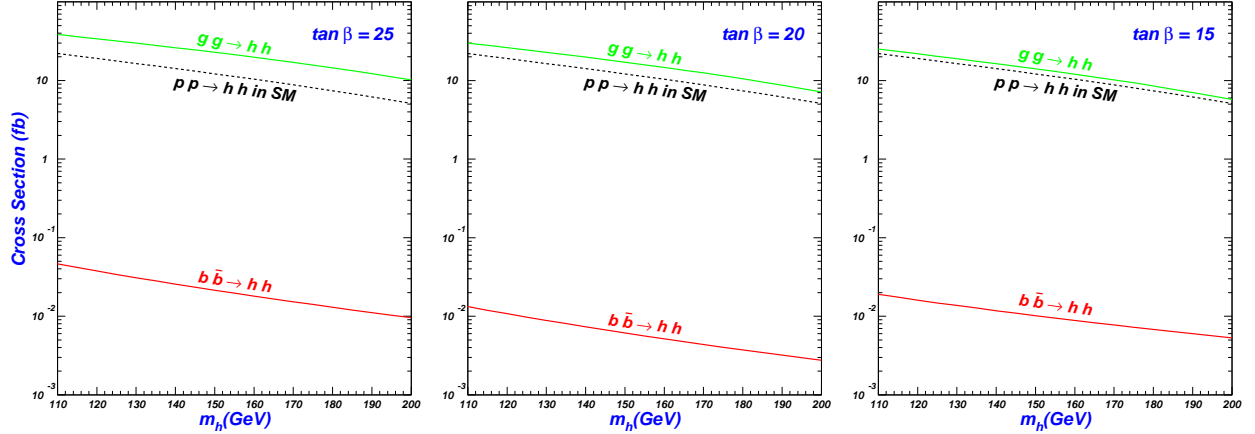


FIG. 6: For  $f = 5.6$  TeV, hadronic cross sections of  $gg \rightarrow hh$  and  $b\bar{b} \rightarrow hh$  at the LHC versus the  $h$  boson mass. The  $pp \rightarrow hh$  process in SM includes  $gg \rightarrow hh$  and  $b\bar{b} \rightarrow hh$ .

over that of  $b\bar{b}$  annihilation process. For  $t_\beta = 25$  and  $35 \text{ GeV} < m_\eta < 75 \text{ GeV}$ , an on-shell  $h$  boson can be produced from the gluon-gluon fusion and  $b\bar{b}$  annihilation, and decays into  $\eta\eta$ . Therefore, the cross sections of the two production processes are enhanced sizably and reach  $\mathcal{O}(10^3 fb)$  and  $\mathcal{O}(10^2 fb)$ , respectively. However, in the parameter space where the  $h$  boson is off-shell, those two cross sections can reach respectively  $\mathcal{O}(10 fb)$  and  $\mathcal{O}(1 fb)$  for  $t_\beta = 25$ , and become smaller for  $t_\beta = 20$  and  $t_\beta = 15$ .

For the  $\eta h$  associated production, the cross sections of gluon-gluon fusion process and  $q\bar{q}$  annihilation process are about in the same order of magnitude, which can reach  $\mathcal{O}(10^2 fb)$  for a light  $\eta$  boson. Our numerical results show the contributions from the process mediated by  $Z$  and  $Z'$  as shown in Fig. 4(a) are dominant for  $q\bar{q} \rightarrow \eta h$ , but in Fig. 3(a) are much smaller than other processes for  $gg \rightarrow \eta h$ . Although the intermediate state  $Z'$  can induce the resonance effects, the contributions from the process mediated by  $Z$  can still dominate over those of  $Z'$  due to the large mass of  $Z'$  and the small branching ratio of  $Z' \rightarrow \eta h$ .

In Fig. 6, we plot the hadronic cross sections of  $gg \rightarrow hh$  and  $b\bar{b} \rightarrow hh$  at the LHC versus the  $h$  boson mass. We find that the cross section of  $b\bar{b} \rightarrow hh$  can be neglected compared with that of  $gg \rightarrow hh$ , and the cross sections of the two processes decrease with increasing of  $m_h$ . Compared with the SM prediction, the cross section of  $hh$  production at LHC in SLHM can be enhanced sizably for a large  $t_\beta$ . For example, with  $f = 5.6$  TeV and  $t_\beta = 25$ , the cross section can be approximately enhanced by 80% for  $m_h = 120 \text{ GeV}$ .

Now we briefly discuss the observable signatures of  $\eta\eta$ ,  $\eta h$  and  $hh$  productions at LHC, respectively. For  $10 \text{ GeV} < m_\eta < 300 \text{ GeV}$ , the  $\eta$  boson mainly decays into  $b\bar{b}$ ,  $\tau\bar{\tau}$  and

$gg$ . The branching ratio of  $\eta \rightarrow \tau\bar{\tau}$  is about 10% of  $\eta \rightarrow b\bar{b}$  [10, 12]. The huge QCD backgrounds make it essentially impossible to discover the signatures  $pp \rightarrow \eta\eta \rightarrow b\bar{b}b\bar{b}$  and  $pp \rightarrow \eta\eta \rightarrow gggg$  at LHC. If one of the double  $\eta$  bosons decays into  $\tau\bar{\tau}$ , and the other decays into  $b\bar{b}$ , the signal to background ratio S/B can be enhanced sizably [30]. Namely,  $pp \rightarrow \eta\eta \rightarrow \tau\bar{\tau}b\bar{b}$  is a promising channel to search for  $\eta\eta$  at LHC. Besides, the rare mode  $pp \rightarrow \eta\eta \rightarrow b\bar{b}\gamma\gamma$  may be also promising since the narrow  $\gamma\gamma$  peak can be reconstructed to distinguish the signal from the backgrounds [30]. Fig. 5 shows that, for  $t_\beta = 15$  and  $t_\beta = 20$ , the cross sections of  $\eta\eta$  production are only several  $fb$  and even less than 1  $fb$ , so it is difficult to search for  $\eta\eta$  at LHC. However, for  $t_\beta = 25$  and  $35 \text{ GeV} < m_\eta < 75 \text{ GeV}$ , the cross sections can reach several thousand  $fb$ , so it is feasible to search for  $\eta\eta$  through  $pp \rightarrow \eta\eta \rightarrow \tau\bar{\tau}b\bar{b}$  at LHC.

For  $m_h < 150 \text{ GeV}$  and  $t_\beta = 25$ , the decay  $h \rightarrow \eta\eta$  is dominant and  $h \rightarrow b\bar{b}$  is subdominant [9, 10, 13]. The largest mode  $pp \rightarrow \eta h \rightarrow \eta\eta\eta$  is interesting, and a detailed study is needed to establish the feasibility of searching for  $\eta h$ . For  $m_h < 150 \text{ GeV}$  and  $t_\beta = 20$  or 15, the dominant decay mode is  $h \rightarrow b\bar{b}$ , and  $h \rightarrow \eta\eta$  is forbidden kinematically. So the promising channel is  $pp \rightarrow \eta h \rightarrow b\bar{b}\tau\bar{\tau}$ . The decay  $h \rightarrow WW$  is dominant for  $m_h > 150 \text{ GeV}$ , and the decay  $h \rightarrow ZZ$  is subdominant for  $m_h > 160 \text{ GeV}$ . Here the largest mode  $b\bar{b}WW$  from the decays  $\eta \rightarrow b\bar{b}$  and  $h \rightarrow WW$  has huge background  $pp \rightarrow t\bar{t} \rightarrow b\bar{b}WW$ , so the mode is not optimistic [31]. The next-largest mode  $b\bar{b}ZZ$  from the decays  $\eta \rightarrow b\bar{b}$  and  $h \rightarrow ZZ$  may be more promising.

Similar to the analysis of  $\eta\eta$  and  $\eta h$  production processes, for  $m_h < 150 \text{ GeV}$  and  $t_\beta = 25$ ,  $pp \rightarrow hh \rightarrow \eta\eta\eta\eta$  is the largest mode, and a detailed study is needed to analyze the signal and the relevant backgrounds. Besides, the promising channels are  $pp \rightarrow hh \rightarrow b\bar{b}\tau\bar{\tau}$  ( $b\bar{b}\gamma\gamma$ ) for  $m_h < 150 \text{ GeV}$  and  $t_\beta = 20$  or 15, and  $pp \rightarrow hh \rightarrow WWWW$  for  $150 \text{ GeV} < m_h < 200 \text{ GeV}$ .

#### IV. CONCLUSION

In the framework of the simplest little Higgs model, we perform a comprehensive study for the pair productions of neutral Higgs bosons at LHC, namely  $gg(b\bar{b}) \rightarrow \eta\eta$ ,  $gg(q\bar{q}) \rightarrow \eta h$  and  $gg(b\bar{b}) \rightarrow hh$ . We find that the cross section of  $gg \rightarrow \eta\eta$  process always dominates over that of  $b\bar{b} \rightarrow \eta\eta$ . The cross sections of the two processes can reach respectively several thousand

$fb$  and several hundred  $fb$  when an on-shell  $h$  boson mediates the two processes. When the  $h$  boson is off-shell, the cross sections of the two processes are reduced by two orders of magnitude, respectively. Besides, the cross sections of  $gg \rightarrow \eta h$  process and  $q\bar{q} \rightarrow \eta h$  process are about in the same order of magnitude, which can reach  $\mathcal{O}(10^2 fb)$  for a light  $\eta$  boson. For the  $hh$  production process at LHC, the cross section in SLHM can be enhanced sizably compared with the SM prediction. The above results imply that it is possible to search for  $\eta$  boson and  $h$  boson through those production processes at LHC. We briefly discuss the observable signatures of  $\eta\eta$ ,  $\eta h$  and  $hh$  at the LHC, and a detailed analysis of the signatures and relevant backgrounds are necessary in the future study.

### Acknowledgment

We thank Shuo Yang and Jin Min Yang for discussions. This work was supported in part by the National Natural Science Foundation of China (NNSFC) under grant No. 11005089, and by the Foundation of Yantai University under Grant No. WL09B31.

### Appendix A: The decay widths of $h$ and $Z'$

In addition to the SM decay modes, the  $h$  boson in the SLHM can decay into  $\eta\eta$  and  $Z\eta$  in the kinematically allowed parameter space. The SLHM corrections to the tree-level decays  $h \rightarrow f\bar{f}$ ,  $WW$ ,  $ZZ$  are mainly from the corresponding modified couplings:

$$\Gamma(h \rightarrow XX) = \Gamma(h \rightarrow XX)_{SM} (g_{hXX}/g_{hXX}^{SM})^2, \quad (A1)$$

where  $XX$  denotes  $WW$ ,  $ZZ$  or fermion pairs. The SM decay width  $\Gamma(h \rightarrow XX)_{SM}$  is obtained using the code Hdecay [32].  $g_{hXX}$  and  $g_{hXX}^{SM}$  are the couplings of  $hXX$  in the SLHM and SM, respectively. The couplings  $g_{hWW}$  and  $g_{hZZ}$  can be found in [10].

The decay rates of  $h \rightarrow gg$  and  $h \rightarrow \gamma\gamma$  are as follows [7]:

$$\Gamma(h \rightarrow gg) = \frac{\alpha_s^2 m_h^3}{32\pi^3 v^2} \left| \sum_f -\frac{1}{2} y_f F_{1/2}(\tau_f) \right|^2, \quad (A2)$$

where  $f = t, T, D, S$ ,  $\tau_f = \frac{4m_f^2}{m_h^2}$  and  $y_f = \frac{v}{m_f} g_{hf\bar{f}}$ .

$$\Gamma(h \rightarrow \gamma\gamma) = \frac{\alpha^2 m_h^3}{256\pi^3 v^2} \left| \sum_f y_f N_{cf} Q_f^2 F_{1/2}(\tau_f) + \sum_V y_V F_1(\tau_V) \right|^2, \quad (A3)$$

where  $y_V = \frac{v}{2m_V^2} g_{hVV}$  with  $V$  denoting the charged gauge bosons  $W^\pm$  and  $X^\pm$ .  $N_{cf}$  and  $Q_f$  are respectively the color factor and the electric charge of the fermion running in the loop. The dimensionless loop factors are

$$F_1(\tau) = 2 + 3\tau + 3\tau(2 - \tau)f(\tau), \quad F_{1/2}(\tau) = -2\tau[1 + (1 - \tau)f(\tau)], \quad (\text{A4})$$

where

$$f(\tau) = \begin{cases} [\sin^{-1}(1/\sqrt{\tau})]^2, & \tau \geq 1 \\ -\frac{1}{4}[\ln(\eta_+/\eta_-) - i\pi]^2, & \tau < 1 \end{cases} \quad (\text{A5})$$

with  $\eta_\pm = 1 \pm \sqrt{1 - \tau}$ .

The decay rates of  $h \rightarrow \eta\eta$  and  $h \rightarrow Z\eta$  are

$$\begin{aligned} \Gamma(h \rightarrow \eta\eta) &= \frac{\lambda'^2 v^2}{8\pi m_h} \sqrt{1 - x_\eta}, \\ \Gamma(h \rightarrow Z\eta) &= \frac{m_h^3}{32\pi f^2} \left(t_\beta - \frac{1}{t_\beta}\right)^2 \lambda^{3/2} \left(1, \frac{m_Z^2}{m_h^2}, \frac{m_\eta^2}{m_h^2}\right), \end{aligned} \quad (\text{A6})$$

where  $x_\eta = 4m_\eta^2/m_h^2$  and  $\lambda(1, x, y) = (1 - x - y)^2 - 4xy$ .

The heavy gauge boson  $Z'$  mainly decays into fermion pairs.

$$\Gamma(Z' \rightarrow f\bar{f}) = \frac{N_{cf}}{24\pi} \sqrt{1 - \tau_f} \left[ \left( (g_L^f)^2 + (g_R^f)^2 \right) \left( 1 - \frac{\tau_f}{4} \right) + \frac{3}{2} g_L^f g_R^f \tau_f \right] m_{Z'}, \quad (\text{A7})$$

where  $g_L^f$  and  $g_R^f$  are from the coupling  $Z' \bar{f} \gamma^\mu (g_L^f P_L + g_R^f P_R) f$ , which can be found in [6, 33].

$$\Gamma(Z' \rightarrow \eta h) = \frac{1}{96\pi} a_{Z'}^2 \left(t_\beta - \frac{1}{t_\beta}\right)^2 \lambda^{3/2} \left(1, \frac{m_\eta^2}{m_{Z'}^2}, \frac{m_h^2}{m_{Z'}^2}\right) m_{Z'}, \quad (\text{A8})$$

where  $a_{Z'} = \frac{m_Z}{f} \frac{\cos \theta_W (1 - \tan^2 \theta_W)}{\sqrt{3 - \tan^2 \theta_W}}$ . Since the coupling is suppressed by  $\frac{v^2}{f^2}$  and without enhancement of  $t_\beta$ , the decay mode  $Z' \rightarrow WW$  is neglected here. The decay modes  $Z' \rightarrow Y^0 Y^0$  and  $Z' \rightarrow X^+ X^-$  are forbidden kinematically [6, 11, 33].

- 
- [1] N. Arkani-Hamed, A. G. Cohen and H. Georgi, Phys. Lett. B **513**, 232 (2001); N. Arkani-Hamed, A. G. Cohen, E. Katz, A. E. Nelson, T. Gregoire and J. G. Wacker, JHEP **0208**, 021 (2002).
  - [2] D. E. Kaplan and M. Schmaltz, JHEP **0310**, 039 (2003); I. Low, W. Skiba, and D. Smith, Phys. Rev. D **66**, 072001 (2002); S. Chang and J. G. Wacker, Phys. Rev. D **69**, 035002 (2004);

- T. Gregoire, D. R. Smith, and J. G. Wacker, Phys. Rev. D **69**, 115008 (2004); W. Skiba and J. Terning, Phys. Rev. D **68**, 075001 (2003); S. Chang, JHEP **0312**, 057 (2003); H. Cai, H.-C. Cheng, and J. Terning, JHEP **0905**, 045 (2009); A. Freitas, P. Schwaller, and D. Wyler, arXiv:0906.1816.
- [3] N. Arkani-Hamed, A. G. Cohen, E. Katz and A. E. Nelson, JHEP **0207**, 034 (2002).
- [4] M. Schmaltz, JHEP **0408**, 056 (2004).
- [5] H. C. Cheng, I. Low, JHEP **0309**, 051 (2003); JHEP **0408**, 061 (2004); H. C. Cheng, I. Low and L. T. Wang, Phys. Rev. D **74**, 055001 (2006); J. Hubisz and P. Meade, Phys. Rev. D **71**, 035016 (2005).
- [6] T. Han, H. E. Logan and L. T. Wang, JHEP **0601**, 099 (2006).
- [7] T. Han, H. E. Logan, B. McElrath, L. T. Wang, Phys. Lett. B **563**, 191 (2003) [Erratum-ibid. B **603**, 257 (2004)].
- [8] C. R. Chen, K. Tobe, C. P. Yuan, Phys. Lett. B **640**, 263 (2006); K. Hsieh, C. P. Yuan, Phys. Rev. D **78**, 053006 (2008); G. A. Gonzalez-Sprinberg, R. Martinez, J-A. Rodriguez, Phys. Rev. D **71**, 035003 (2005); L. Wang, et al., Phys. Rev. D **75**, 074006 (2007); Phys. Rev. D **77**, 015020 (2008); Phys. Rev. D **79**, 055013 (2009); R. S. Hundi, B. Mukhopadhyaya, A. Nyffeler, Phys. Lett. B **649**, 280 (2007); P. Kai, et al., Phys. Rev. D **76**, 015012 (2007); C. X. Yue, N. Zhang, Europhys. Lett. **77**, 51003 (2007); S. Yang, Phys. Lett. B **675**, 352-355 (2009).
- [9] L. Wang, F. Xu, J. M. Yang, JHEP **1001**, 107 (2010).
- [10] K. Cheung and J. Song, Phys. Rev. D **76**, 035007 (2007).
- [11] K. Cheung, J. Song, P. Tseng and Q.-S. Yan, Phys. Rev. D **78**, 055015 (2008).
- [12] W. Kilian, D. Rainwater and J. Reuter, Phys. Rev. D **71**, 015008 (2005).
- [13] X. F. Han, L. Wang, J. M. Yang, Nucl. Phys. B **825**, 222 (2010).
- [14] C. Dib, R. Rosenfeld, A. Zerwekh, JHEP **0605**, 074 (2006); J. J. Liu, et al., Phys. Rev. D **70**, 015001 (2004); L. Wang, W. Y. Wang, J. M. Yang, H. J. Zhang, Phys. Rev. D **76**, 017702 (2007).
- [15] N. Brambilla, et al. (Quarkonium Working Group), arXiv:hep-ph/0412158; W. M. Yao, et al. (Particle Data Group), J. Phys. G **33**, 1 (2006); R. Balest, et al. (CLEO Collaboration), Phys. Rev. D **51**, 2053 (1995).
- [16] A. A. Barrientos Bendezu, Bernd A. Kniehl, Phys. Rev. D **64**, 035006(2001); T. Plehn, M. Spira and P. M. Zerwas, Nucl. Phys. B **479**, 46(1996); A. Djouadi, W. Kilian, M. Muhlleitner

- and P. M. Zerwas, Eur. Phys. Jour. C **10**, 45(1999); A. Belyaev, Manuel Drees, Oscar J. P. Eboli, J. K. Mizukoshi, S. F. Novaes, Phys. Rev. D **60**, 075008(1999); A. Belyaev, M. Drees and J. K. Mizukoshi, Eur. Phys. Jour. C **17**, 337(2000); R. Lafaye, D. J. Miller, M. Muhlleitner and S. Moretti, hep-ph/0002238; M. Moretti, S. Moretti, F. Piccinini, R. Pittau, JHEP 0502, 024(2005).
- [17] H. de Sandes, R. Rosenfeld, Phys. Lett. B **659**, 323(2008); P. K. Das and B. Mukhopadhyaya, hep-ph/0303135.
- [18] W. Ma, C.-X. Yue, Y.-Z. Wang, Phys. Rev. D **79**, 095010 (2009).
- [19] G. 't Hooft and M. J. G. Veltman, Nucl. Phys. B **153**, 365 (1979).
- [20] T. Hahn and M. Perez-Victoria, Comput. Phys. Commun. **118**, 153 (1999); T. Hahn, Nucl. Phys. Proc. Suppl. **135**, 333 (2004).
- [21] J. S. Bell and R. Jackiw, Nuovo Cimento A **60**, 47 (1969).
- [22] C. Liu, S. Yang, Phys. Rev. D **81**, 093009 (2010).
- [23] J. Pumplin, et al., JHEP **0602**, 032 (2006).
- [24] Tevatron Electroweak Working Group, CDF, D0 Collaborations, arXiv:1007.3178.
- [25] C. Amsler, et al., Phys. Lett. B **667**, 1 (2008).
- [26] R. Barate, et al. (LEP Working Group for Higgs boson searches), Phys. Lett. B **565**, 61 (2003).
- [27] A. G. Dias, C. A. de S. Pires, P. S. Rodrigues da Silva, Phys. Rev. D **77**, 055001 (2008); A. Gutierrez-Rodriguez, Mod. Phys. Lett. A **25**, 703-713 (2010).
- [28] J. I. Illana, M. D. Jenkins, Acta Phys. Polon. B **40**, 3143 (2009).
- [29] F. d. Aguila, J. I. Illana, M. D. Jenkins, arXiv:1007.3573.
- [30] U. Baur, T. plehn, and D. Rainwater, Phys. Rev. D **68**, 033001 (2003); Phys. Rev. D **69**, 053004 (2004).
- [31] D. rainwater, arXiv:hep-ph/0702124.
- [32] A. Djouadj, J. Kalinowski and M. Spira, Computl. Phys. Commun. **108**, 56 (2006).
- [33] P. Kalyniak, D. Tselikhovich, arXiv:0903.4739.